FMOS Spectroscopic Follow-up on Large Scale Structures around Distant Clusters Traced by PISCES

Tadayuki Kodama[1] and the PISCES team
[1]*National Astronomical Observatory of Japan, Mitaka, Tokyo 181–8588, Japan*

Abstract

We are conducting the PISCES project, a systematic study of 15 distant clusters at $0.4 < z < 1.3$ using the unique wide-field ($30'$) optical camera Suprime-Cam mounted on the prime focus of Subaru telescope. The main objectives of this project are twofold: (1) Mapping out the large scale structures in and around the clusters on 10-14 Mpc scale to study the hierarchical growth of clusters through assembly of surrounding groups. (2) Investigating the environmental variation of galaxy properties along the structures to study the origin of the morphology-density and star formation-density relations.

FMOS, which has a comparable field of view of $30'$ to Suprime-Cam, will be an excellent facility to follow-up the PISCES project in two reasons. Firstly, we can spectroscopically confirm the structures traced by the photometric redshift technique which tends to suffer from the projection effect in the low density regions. Secondly, we can measure the on-going star formation rates along the structures using Hα line intensity, and hence directly detect the truncation of star formation during the course of galaxy assembly to denser regions.

1 Panoramic Imaging and Spectroscopy of Cluster Evolution with Subaru (PISCES)

PISCES is a panoramic imaging survey of distant clusters using the Subaru wide-field optical camera Suprime-Cam which provides $34'\times27'$ field of view corresponding to a physical area of 16×13 Mpc^2 at $z \sim 1$. This long term project has started since 2003, and we aim to target 15 X-ray selected distant clusters in total at $0.4 \lesssim z \lesssim 1.3$, in good coordination with *ACS/HST*, *XMM*, and *Chandra* observations. The goals of this programme is to map out the large scale structures around clusters to trace the cluster assembly history and then to look into the galaxy properties as a function of environment along the structures to directly identify the environmental effects acting on galaxies during their assembly to higher density regions.

This unique project is currently underway and some preliminary results on the large scale structures are shown in Figs. 1 and 2. These two rich clusters at z=0.55 and 0.83 are imaged in multi optical bands with Suprime-Cam, and photometric redshifts [17] have been applied to efficiently remove foreground/background contaminations and isolate the cluster member candidates (cf., [18]). Many substructures are now clearly seen around the main body of

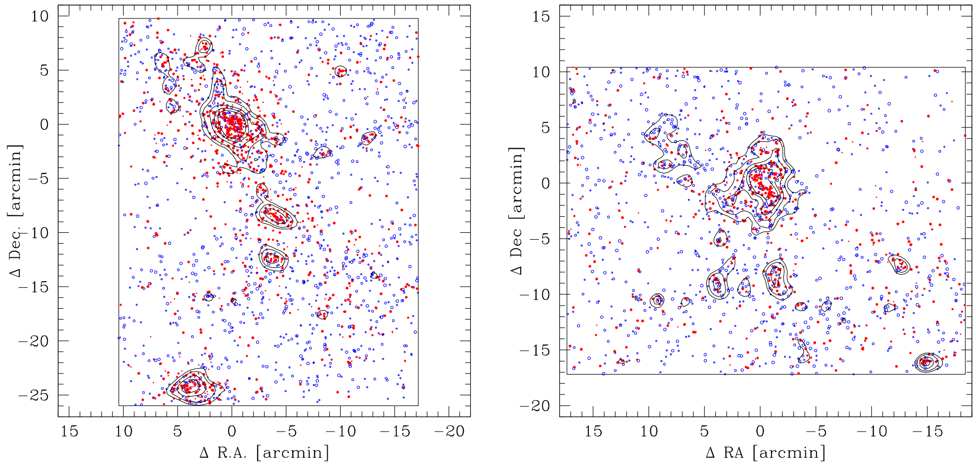

Figure 1: The panoramic maps of CL0016+16 cluster (z = 0.55; left panel) and RXJ0152.7–1357 (z=0.83; right panel) 10 arcminutes corresponds to physical scales of 3.8 Mpc and 4.6 Mpc, respectively. Using photometric redshift technique based on multi-colour data ($BVRi'z'$ and $VRi'z'$, respectively), plotted are the photometric member candidates selected with redshift cuts of $0.50 \le z \le 0.58$ and $0.78 \le z \le 0.86$, respectively. Contours show local 2-D number density of galaxies at 1.5, 2, 3, 4, 5 σ above the mean density. Coordinates are shown relative to the centre of the main cluster. Large scale filamentary structures (>10Mpc) are seen in both clusters.

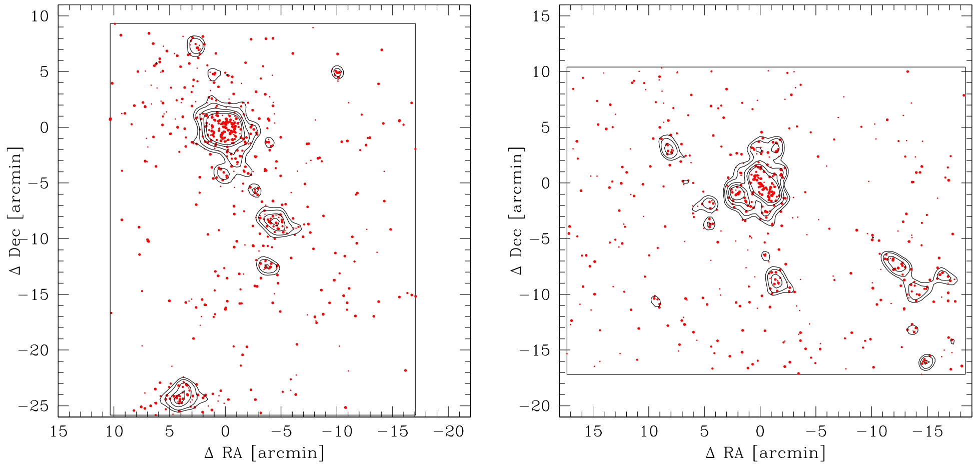

Figure 2: The same as Figure 1, but only red galaxies on the colour-magnitude sequence are shown rather than phot-z selected galaxies. The red galaxies are selected on the basis of VRi' colours for CL0016 and $Ri'z'$ colours for RXJ0153, respectively, and some red colour slice cuts are applied to isolate the passively evolving galaxies at cluster redshifts. This technique gives narrower redshift slice ($\Delta z \sim 0.05$) hence has less projection effect, but are biased to redder populations. It is therefore complemental to the phot-z slice technique.

the clusters which tend to be aligned in filamentary structures extending to >10 Mpc scale across. Although these structures should be confirmed spectroscopically later on, these already provide good evidence for cluster assembly in the hierarchical Universe.

[18] have presented the environmental dependence of galaxy colours along the filamentary structures around the A851 cluster (z=0.41). They have shown that the galaxy colours change rather sharply at relatively low density regions such as galaxy groups along the filaments well outside of the cluster core. Together with the similar findings in the local Universe [22][12]. the environmental effects that truncate star formation are not the cluster specific mechanism such as ram-pressure stripping [1] but are found to be much wider spread into low density regions. We should therefore pay greater attention to galaxy group as a key hierarchy for the environmental effects and should identify what is happening on galaxies in there. It is also important to extend this analysis to higher redshifts as the galaxy environment is expected to change dramatically during the course of vigorous assembly, which is probably related to the appearance of morphology-density relation [9].

2 FMOS roles for PISCES

2.1 Identifying the large-scale substructures and measuring the dynamical mass of the groups

First of all, taking as many spectra as possible from the photometrically identified large scale structures is crucial to prove their reality, since our photometric approach may well suffer from the projection effect along the line of site due to the broad phot-z slice cuts, as we go to lower density regions. Importantly, Hα line comes to FMOS window (0.9μm<λ<1.8μm) for $0.4 < z < 1.7$, covering the entire redshift range of our current PISCES targets. Not only definitively removing the foreground/background contamination and identifying the physically associated real groups, spectroscopic redshifts of individual cluster members will also provide us two critical information: (1) Dynamical mass of the systems which can then be compared to lensing mass and the X-ray mass to address the dynamical state of the systems. (2) 3-D velocity structures, providing the recent and/or near future cluster-cluster/cluster-group merger histories.

2.2 Identifying the physical mechanisms behind the environmental effects and measuring environmentally dependent cosmic star formation histories

Hα will offer one of the best measures of on-going star formation rate of galaxies, since its much less affected by dust extinction or metallicity variation, unlike the OII line or UV flux that are commonly used at high redshifts [14]. Therefore we can directly identify when, where and on what timescale the star formation is truncated as the galaxies/groups fall into clusters along the filaments (Fig. 3).

It is also notable that the Hβ, OIII and Mg_2 lines also come into the FMOS window for the high redshift clusters of our PISCES targets ($z \gtrsim 0.8$). Since different spectral features are sensitive to different stellar ages [14], we can resolve the recent star formation histories in fine time scales by combining the individual information [4][23] The emission line (Hα) will measure the amplitude of on-going star formation (10^7 yrs), while the Balmer absorption line (eg., Hβ; E+A [10][7]) give the luminosity (mass) contribution from the stars formed immediately before the truncation (10^{8-9} yrs). The 4000Å break, Mg_2, and broad-band colours specify the features of longer-lived populations ($>10^9$ yrs) [19]. In this way we can trace back the star formation histories in the individual galaxies from 10^7 yrs to $>10^9$ yrs from the observed epoch. Resolving the 'recent' star formation histories in galaxies in the transition regions (groups) is the key to understanding the physical processes behind the truncation. In particular, strong Hα emission is seen in the star-bursting phase, supporting galaxy-galaxy mergers, and very strong Balmer absorption line (E+A feature) will follow in the post star-burst phase. If the star formation is more gradually truncated ($\gtrsim$1Gyr) due to halo gas stripping (strangulations), we won't see any excess of E+A features [4].

By integrating the star formation rates within clusters and scaling them by the mass of the clusters, one can obtain a global star formation history in clusters as illustrated in Fig. 3. This is somewhat equivalent to the Butcher-Oemler plot showing the increase of blue galaxy fraction in clusters with redshift [6].

2.3 Identifying the evolutionary stage of faint blue galaxies seen in down-sizing effect

It is known that the galaxy properties depend on mass or luminosity as well. Using the SDSS data, [13][2] have shown an interesting break mass at $3\times10^{10}\mathrm{M}_\odot$ above which the dominant population is red passively evolving galaxies, while below that mass the contribution of blue active galaxies become dominant. Galaxy morphologies are also known to be luminosity (or stellar mass) dependent [24]. This indicates that the formation of massive galaxies and less massive galaxies are quite different, in the sense that massive galaxies form early in the Universe, while dwarf galaxies form later on average or still forming stars at present. This is referred to as "down-sizing" in galaxies that host star formation [8].

As we look back higher redshift Universe, we expect to approach the formation epoch of more massive galaxies. Here we investigate the galaxy colours at $z \sim 1$ as a function of luminosity (or stellar mass) utilizing the unique Suprime-Cam imaging data-set ($BRi'z'$) on the Subaru/XMM-Newton Deep Survey (SXDS). These data are both sufficiently deep (z'_{AB}=25, 6-10σ) and wide (1.2 deg^2), which enable us for the first time to investigate the photometric properties of statistical sample of galaxies at $z \sim 1$ down to $\sim M^*$+3 with

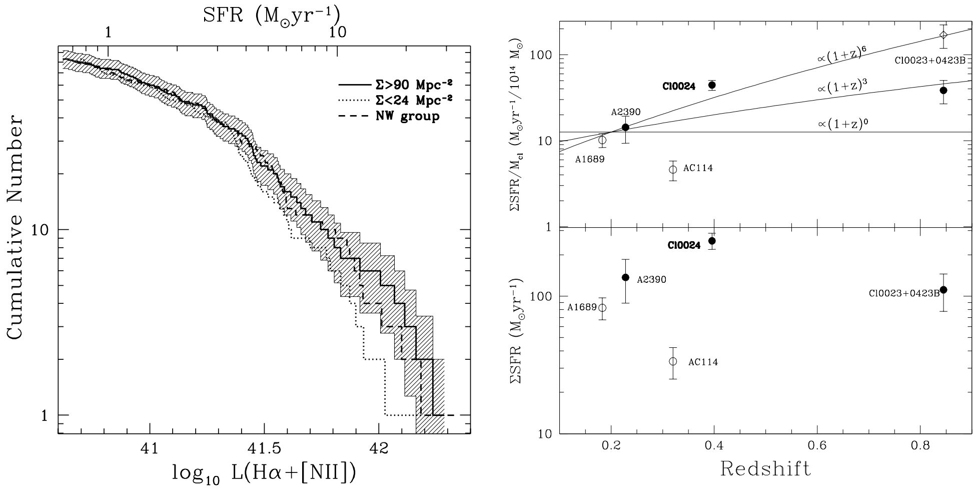

Figure 3: *Left panel:* Hα luminosity functions separated into three environments; high-density, low-density, and a NW group of CL0024 cluster based on the Subaru wide-field narrow-band imaging [21]. The shape of luminosity functions is broadly unchanged with environments, suggesting the rapid truncation of star formation. *Right panel:* The total SFR within 0.5 R_{200}, is shown as a function of redshift for CL0024 and four other clusters with deep Hα observations [11][21]. We show the total SFR within $0.5R_{200}$ divided by the total mass M_{200}, for the same clusters. The diamond symbol shows the effect of assuming the dynamical mass estimate for CL0023 (see [21] in detail). The solid lines shows different scalings with $(1+z)$, as a guide.

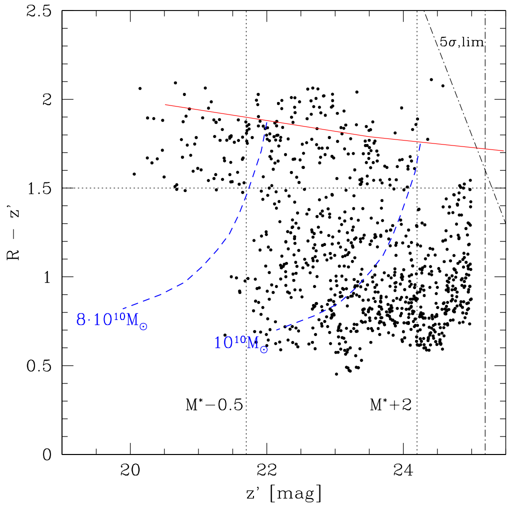

Figure 4: Field-corrected colour-magnitude diagram for the $z \sim 1$ galaxies in high density regions in SXDS [20]. The solid line show the expected location of colour-magnitude sequence at $z \sim 1$ assuming a passive evolution with $z_{\rm form}$=5 [16]. The deficit of both blue galaxies at the bright/massive end and the deficit of red galaxies at the faint/less-massive end are both clearly identified.

respect to the passive evolution. We first identify five $z \sim 1$ high density regions by applying colour cuts at $1.7<R-z'<2.0$ and $0.8<i'-z'<1.1$, which correspond to the colours of passively evolving galaxies at $z \sim 1$ [16]. We then combine these five regions (amounting to 141 arcmin^2 in total) and subtract off the low density regions at $z \sim 1$ (scaled to the same area) on the colour-magnitude diagram to isolate only $z \sim 1$ galaxies in a statistical sense. This field subtraction should work since both regions are expected to have the same amount of foreground/background contaminations.

The field-corrected colour-magnitude diagram thus constructed for $z \sim 1$ galaxies in high density regions is shown in Fig. 4. Most striking feature on this diagram is that there are two distinct populations, 'bright+red' and 'faint+blue'. More precisely, we show a deficit of red and faint galaxies below M^*+2 or $10^{10}\mathrm{M}_\odot$ in stellar mass and a lack of blue massive galaxies above $M^*-0.5$ or $8\times10^{10}\mathrm{M}_\odot$ in stellar mass. This indicates again the down-sizing in galaxy formation, where star formation in massive galaxies take place early in the Universe and is already truncated, while that in less massive systems is generally slow and is still on-going at the observed epoch [20].

Why are the faint galaxies always blue? Is that because they are just forming? Or do they have much extended star formation over the long period of time? To separate out these two possibilities, the key quantity to measure is the so-called birth-rate parameter (b) of these faint blue galaxies **??**. Here b' is re-defined as on-going star formation rate divided by integrated stellar mass of the system ($b'=SFR/\mathrm{M}^*$). SFR can be derived from Hα line intensity while M^* can be obtained from the longest wavelength data that is available. This parameter describes what phase of star formation each galaxy is in, and therefore can discriminate between genuinely young galaxies formed recently (large b') and star forming galaxies formed long time ago (small b').

It is also interesting to directly detect the brightening of the break luminosity or mass with increasing redshift [19] by going even higher redshifts. Hα can be detectable out to $z \sim 1.7$ with FMOS.

We have assumed the cosmological parameters of (H_0, Ω_m, Ω_Λ)=(70, 0.3, 0.7), throughout this paper.

We acknowledge to the SXDS team (Kaz Sekiguchi et al.). This work was financially supported in part by a Grant-in-Aid for the Scientific Research (No. 15740126) by the Japanese Ministry of Education, Culture, Sports and Science.

References

[1] Abadi, M.G., Moore, B., Bower, R.G., 1999, MNRAS, 308, 947

[2] Baldry I. K., et al., 2004, ApJ, 600, 681

[3] Balogh, M.L., et al., 2001, ApJ, 557, 117

[4] Balogh M.L., et al., 1999, ApJ, 527, 54

[5] Baugh, C.M., et al., 2002, astro-ph/0203051

[6] Butcher, H., Oemler, A., 1984, ApJ, 285, 426

[7] Couch, W. J., Sharples, R. M., 1987, MNRAS, 229, 423

[8] Cowie, L.L., Songaila, A., Hu, E.M., Cohen, J.G., 1996, AJ, 112, 839

[9] Dressler, A., 1980, ApJ, 236, 351

[10] Dressler, A., Gunn, J. E., 1992, ApJS, 78, 1

[11] Finn, R.A., Zaritsky, D., McCarthey, D.W., 2004, ApJ, 604, 141

[12] Gómez, P.L., et al., 2003, ApJ, 584, 210

[13] Kauffmann, G., et al., 2003, MNRAS, 341, 54

[14] Kennicutt, R.C., et al., 1994, ApJ, 435, 22

[15] Kennicutt, R.C., 1988, ARA&A, 36, 189

[16] Kodama, T., et al., 1998, A&A, 334, 99

[17] Kodama, T., Bell, E.d F., Bower, R.G., 1999, MNRAS, 302, 152

[18] Kodama, T., et al., 2001, ApJ, 562, L9

[19] Kodama, T., Bower, R.G., 2001, MNRAS, 321, 18

[20] Kodama, T., et al., 2004, MNRAS, in press

[21] Kodama, T., Balogh, M.L., et al., 2004, in prep.

[22] Lewis, I., et al., 2002, MNRAS, 334, 673

[23] Poggianti, B.M. et al. 1999, ApJ, 518, 576

[24] Treu, T., et al., 2003, ApJ, 591, 53